Magnetic, structural, and electronic properties of Co doped Fe/MgO interface: Density functional approach

Nurul Ikhsan[a,b], Yuusaku Taguchi[a], Masao Obata[a], Makoto Nakamura[a], Suprijadi[b], Tatsuki Oda[a,c]

[a]Graduate School of Natural Science and Technology, Kanazawa University, Kakuma, Kanazawa 920-1192 Japan, E-mail: ikhsan@cphys.fi.itb.ac.id
[b]Faculty of Mathematics and Natural Sciences, Institut Teknologi Bandung, Jl. Ganesha 10, Bandung 40132 Indonesia
[c]Institute of Science and Engineering, Kanazawa University, Kakuma, Kanazawa 920-1192 Japan, E-mail: oda@cphys.s.kanazawa-u.ac.jp

Abstract We performed ab-initio electronic structure calculation in Co doped Fe/MgO interface on the basis of density functional theory. Two different slab models are considered, depending on the place of Co atom; at the interface and in the Fe layer. With using atomic forces, we obtained the optimized structure at the interface and discussed the layer distance of interface and the local structure around Co. Spin magnetic moments on Fe and Co atoms are also discussed. In the band dispersion at the Fermi level, distribution of the angular orbital component shows the possibility of perpendicular magnetic anisotropy.
Keywords: Fe/MgO interface, magnetic anisotropy energy, MRAM, density functional theory

1 Introduction

The Fe/MgO interface is well known as magnetic tunnel junction (MTJ) in magnetic random access memory (MRAM). Current technology of MTJ has the limitation for high density memory due to in-plane magnetization properties. Also large spin polarized currents are required in order to reverse the magnetization in spin-transfer-torque MRAM. Fortunately, recent works on Fe/MgO interface have alternatives for this problem, such as perpendicular magnetization or electric field assisted magnetization reversal. Experimental and theoretical works [1, 2, 3, 4, 5] have proved that this interface is one of the promising candidates for low powered memory devices, e.g. MRAM.

Maruyama *et al.* successfully showed that electric field can cause large MAE change in Fe/MgO junction [1]. Later Shiota *et al.* also confirm magnetization control by electric field on FeCo/MgO interface [2]. The CoFeB/MgO interface with large tunnel magneto resistance has successfully grown by Ikeda *et al.* [3], which is very interesting for devices application. Last two experiments used Co doping instead of pure Fe for magnetic materials such as FeCo [2], FeCoB [3]. These experiments are also supported by the theoretical work [5] on FeCo monolayer which concludes that MAE can be modified by changing the number of valence electrons, such as Co doping. Based on this comparative result between experimental and theoretical view, we have investigated the effect of Co atom in Fe/MgO interface by first-principles calculation based on the spin polarized density functional theory. In this study, we consider two models of Co impurity placement; one at the interface and other in the Fe layer. We found that, when Co is at interface instead of Fe, Co is slightly drawn into the Fe substrate and that the analysis of angular orbital components of Fe implies contributions to the perpendicular magnetic anisotropy energy. We will present spin magnetic moments, density of states, and band dispersions.

Table 1: Averaged Fe-O distance(Å) at FeCo/MgO interfaces.

System	a_{MgO}(L)	a_{Fe}(S)	Others
MgO/Fe_3Co/Fe (model A)	2.179	2.161	
MgO/Fe/Fe_3Co/Fe (model B)	2.187	2.161	
MgO/Fe/Au			2.16[a]
MgO/Fe/Pt			2.31[b]
MgO/Fe	2.09[c]		
MgO/Fe/Au	2.08[c]		
Fe/MgO/Fe	2.30[d]		

[a] Au in-plane lattice constant [4]
[b] Pt in-plane lattice constant [4]
[c] ref. [11]
[d] ref. [12]

2 Model and method

This work takes two minimum slab models; MgO(3ML)/Fe_3Co(1ML)/Fe(2ML) and MgO(3ML)/Fe(1ML)/Fe_3Co(1ML)/Fe(1ML) (both are 36 atoms in 2×2 in-plane supercell configuration), as shown in Fig. 1. In the former, the Co atom is placed at the interface (model A), and in the latter, at the inside of Fe layers (model B) (see Figs. 1 (a) and (b)). We call all the magnetic atoms (Fe and Co) with numbers, starting from 1 until 12, atom number 1 until 4 are located at the interface as shown in Fig. 1 (c), then atom number 5 until 8 at the second Fe layer, finally atom number 9 until 12 at the bottom layer of system. The Co atom is occupied at atom number 4 and 5 for the first (model A) and second (model B) slabs, respectively. Although the interface Fe/MgO has been fabricated in experiment, the in-plane lattice constant has not been determined even in the clean interface. Therefore, for these slab models, two different in-plane lattice constants 5.74Å (= a_{Fe}) and 5.94Å (= a_{MgO}), which correspond to the bulk lattice constants of Fe and MgO respectively. There is a lattice constant difference by 3.4%. S and L suffixes are given for small (Fe) and large (MgO) lattice constants, respectively, and totally we have four slab models.

For these models, we have carried out first principles calculation which employs the density functional theory [6] and ultra-soft pseudopotential [7]. Energy cutoffs for electron density and wavefunction are 300Ry and 30Ry respectively [8]. Here we used the 4x4x1 mesh of **k** space sampling. The generalized gradient approximation [9] was adopted for exchange correlation energy. In this work, the calculation is within a collinear magnetic scheme. We optimized electronic wavefunctions and atomic positions by minimizing the total energy functional. The structural optimization has been performed by using atomic forces except for the in-plane lattice constant. The ESM method [10] with zero external electric field condition was used to avoid artificial built-in electric field in this repeated slab model; ESM/vacuum/slab/vacuum. For both vacuum layers, the width of 5.29Å is taken. The atomic magnetic moment is estimated by integrating the spin density in the atomic sphere with the radius (0.9Å for magnetic atoms).

3 Result and Discussion

We obtained the optimized structure after all the atomic forces reach equilibrium. Table 1 shows details of the optimized interface distance compared to related works. We obtained distances of

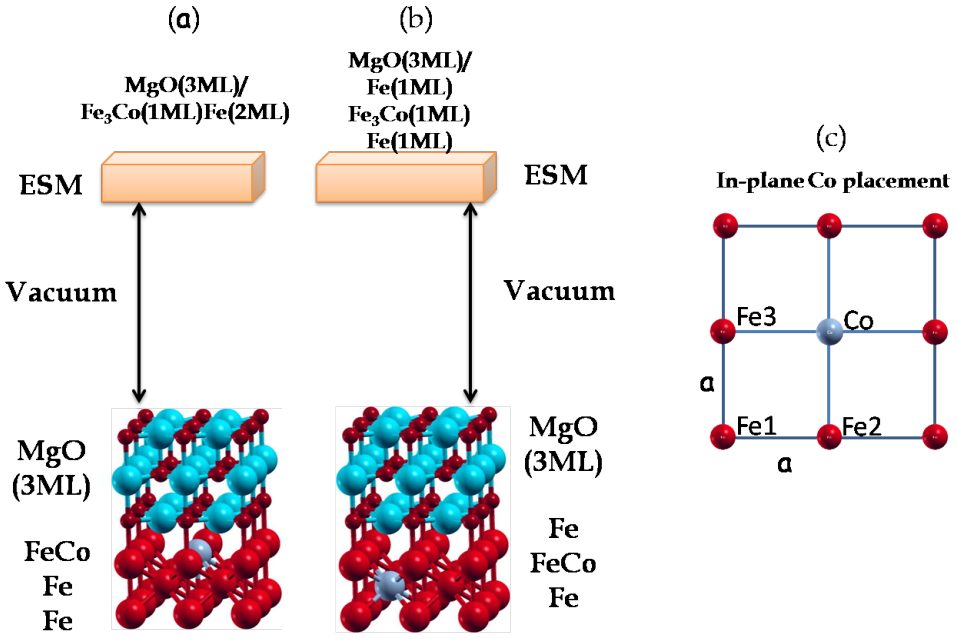

Figure 1: Fe_3Co/MgO interface model with different Co placement: (a) (model A) Co at the interface, (b)(model B) Co in the middle of Fe layer, (c) in-plane view of magnetic layer in model A.

2.18Å and 2.16Å for model A with a_{MgO} and a_{Fe} lattice constants, respectively. In these results we observe that the smaller lattice constant produces smaller interface distance. As another interesting point, as shown in Fig. 2, we found that the Co atom moved from the Fe layer to the magnetic substrate by 0.03Å and 0.04Å for the model A with a_{MgO} and a_{Fe}, respectively. Even when we put the Co in the middle of Fe layer, as indicated in Fig. 3, still we observed slight contracting distortion of Co to the Fe layer. From these behaviors, we may deduce that Co prefers to be surrounded by Fe. We also observed that the model B has a slightly lower total energy than the model A by 3meV, implying that Co impurities in the middle Fe layer provides more stable system than those at the interface.

The total magnetization and atomic magnetic moments are listed in Table 2. We observed that the Fe magnetic moment at interface, whose average is $2.8\mu_{\mathrm{B}}$, is much enhanced from the value of second magnetic layer, the bulk value ($2.2\mu_{\mathrm{B}}$) [13], and the experimental value in the nano clusters [14]. In contrast of this enhancement, the Co magnetic moments are similar to $1.8\mu_{\mathrm{B}}$. Based on the discussion in the previous work [12], the enhancement on Fe magnetic moment is not attributed to the charge transfer to the oxygen at interface, but is understood as surface properties of Fe layer. Indeed, the Co magnetic moment has a similar value obtained by the monolayer model [15]. At surface, electron wavefunction can be localized due to the lack of electron transfer to the open space while the electron transfer to the neighbors make the wavefunction delocalized in the bulk. This localized electron contributes to larger magnetic moment. Electrons at interface are also easier to be localized compared to the middle layer and therefore, such interface accommodates the magnetic atom to a larger magnetic moment. Discussion mentioned above on delocalized electron also explains the smaller magnetic moment at the smaller lattice constant (see Table 2).

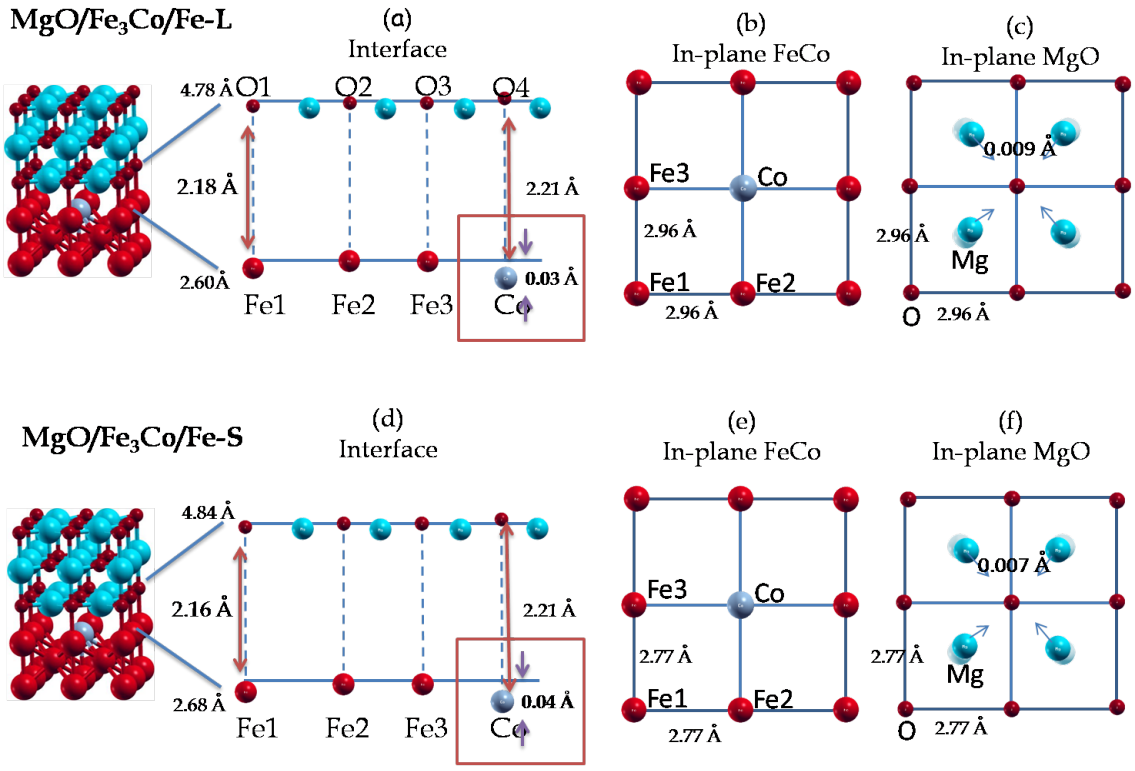

Figure 2: Optimized structure of model A, with large [(a), (b), (c)] and small [(d), (e), (f)] lattice constant. Co movement was found in all models.

Table 2: Total magnetization and atomic magnetic moment of all Fe and Co atoms.

	Mag. Mom.(μ_B) Co:interface			Mag. Mom.(μ_B) Co:in-layer	
	(L)	(S)		(L)	(S)
Total	33.50	33.40	Total	33.60	32.21
Fe 1	2.87	2.84	Fe 1	2.87	2.82
Fe 2	2.86	2.82	Fe 2	2.87	2.82
Fe 3	2.86	2.82	Fe 3	2.87	2.82
Co	1.85	1.81	Fe 4	2.87	2.82
Fe 5	2.55	2.50	Co	1.84	1.83
Fe 6	2.55	2.50	Fe 6	2.48	2.44
Fe 7	2.55	2.50	Fe 7	2.48	2.44
Fe 8	2.55	2.50	Fe 8	2.49	2.45
Fe 9	2.97	2.95	Fe 9	2.96	2.94
Fe 10	2.97	2.95	Fe 10	2.96	2.94
Fe 11	2.97	2.95	Fe 11	2.96	2.94
Fe 12	2.97	2.95	Fe 12	2.96	2.94

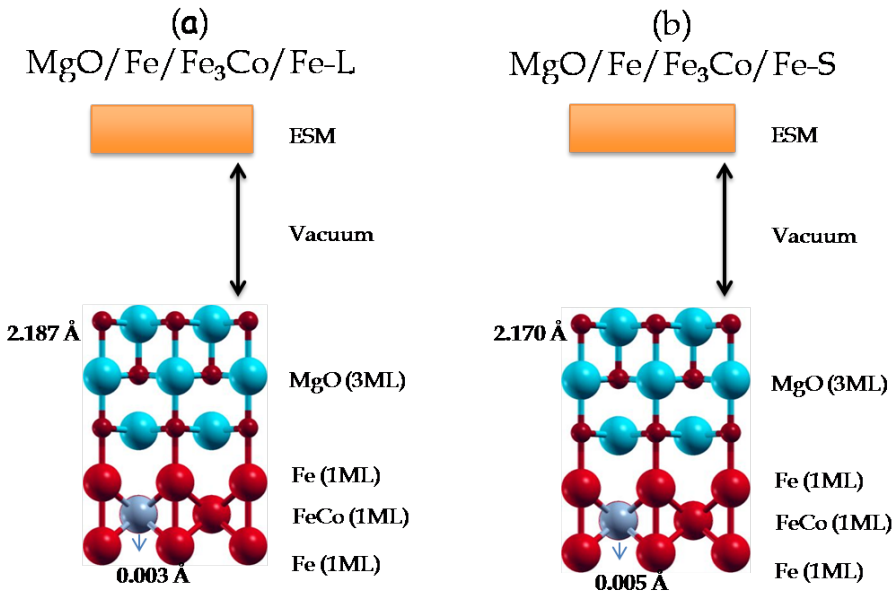

Figure 3: Optimized structure of model B with small (a) and large (b) lattice constant, Co atom slightly moved in -z direction.

Fig. 4 shows the partial density of states (DOS) on Co and Fe atoms at the first and second magnetic layers with the smaller lattice constant (a_{Fe}). At interface, DOS's near the Fermi level on Fe's mainly come from minority spin states, while in the middle layer, those on Fe's are not so large. The latter is a consequence of the splitting that some parts of states around the Fermi level are made lowered and raised to the occupied and unoccupied energy regions, respectively. Such behavior is consistent with the smaller magnetic moment in the middle layer. Similar to the case of Fe, there is larger Co DOS around the Fermi level at interface than in the middle layer. Compared with Fe, we observe smaller exchange splitting in the Co DOS. This observation corresponds that the Co magnetic moment is smaller than Fe. In Fig. 5, the orbital-separated contribution is depicted for both magnetic atoms (Fe1 at interface and Co). The partial DOS from each angular orbital component in Fig. 4 shows that in the near Fermi level there is a large contribution from $3\mathrm{d}_{xy}$, $3\mathrm{d}_{zx}$, $3\mathrm{d}_{yz}$, and $3\mathrm{d}_{x^2-y^2}$ orbitals. These four angular orbital components in vicinity of the Fermi level hold important role to the magnetic anisotropy at the interface, as discussed in the later paragraph.

Magnetic anisotropy energy (MAE) is the internal characteristic of magnetic materials, which can be estimated from the total energy difference between out-of-plane and in-plane magnetizations. The contribution of MAE comes from magnetostatic dipole-dipole interaction and electronic structures around the Fermi level. When considering the situation involved in a practically applied electric field, MAE change in the dipole contribution may be negligible due to few variation of magnetic moment. Here we consider the contribution from spin-orbit interaction, which can be

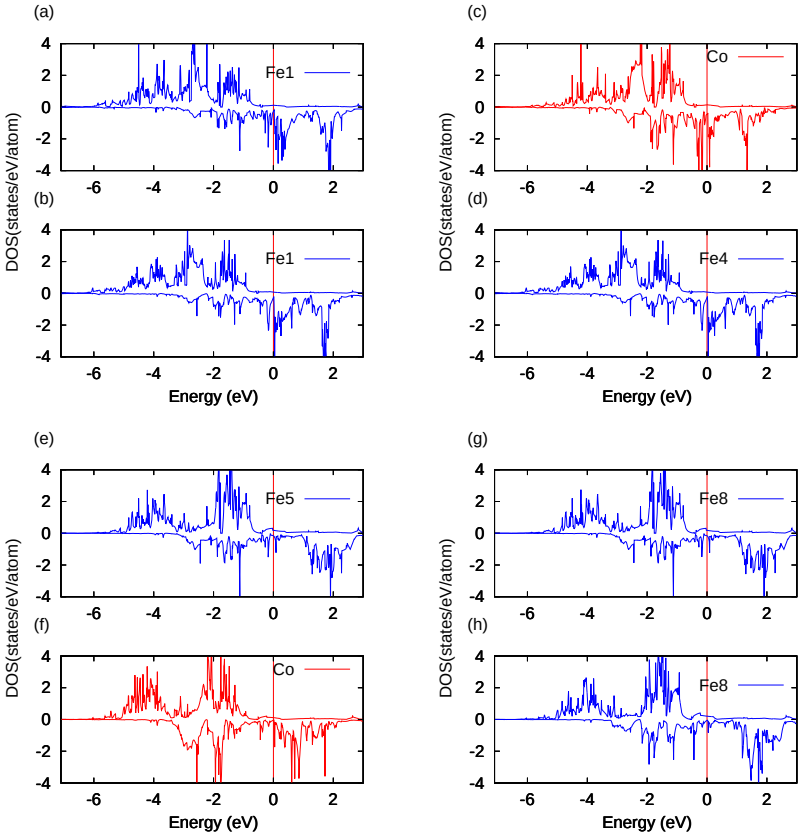

Figure 4: Partial density of states on magnetic atoms (Fe and Co) in models A and B with smaller lattice constant (a_{Fe}) : (a) A Fe1, (b) B Fe1, (c) A Co, (d) B Fe4, (e) A Co, (f) B Fe5, (g) A Fe8, (h) B Fe8. The solid (red) and dashed (blue) curves represent Co and Fe atoms, respectively, and the upper and lower panels indicate spin-up (majority), and spin-down (minority) states.

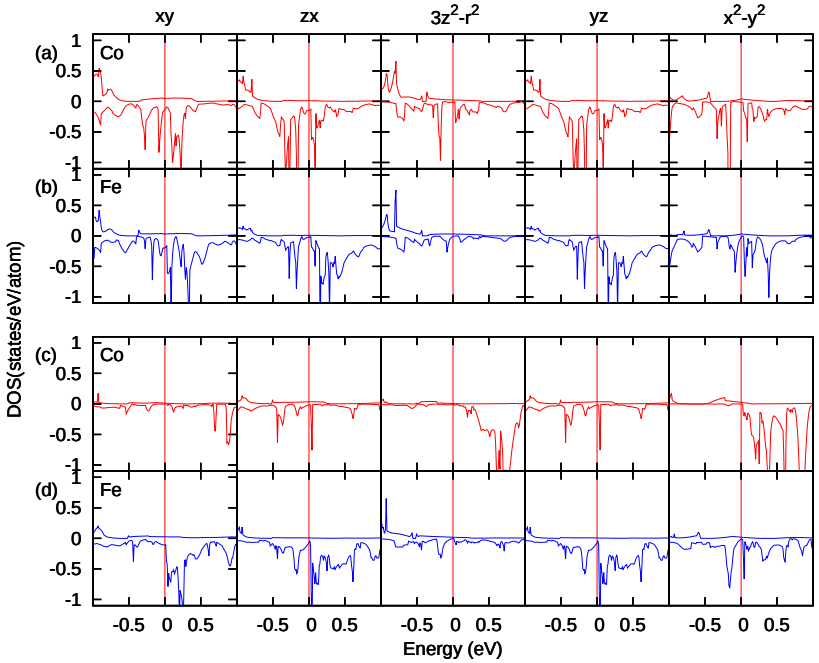

Figure 5: Partial density of states (PDOS) of (a) Co and (b) Fe1 in model A with a_{Fe}, also PDOS of (c) Co and (d) Fe1 atom in model B with a_{Fe}. The solid (red) and dashed (blue) curves represent Co and Fe, respectively.

represented with the second order perturbation theory as follows [16],

$$\mathrm{MAE} \propto \sum_{\mathbf{k}} \sum_{o,u} \frac{|\langle \mathbf{k}, o | l_z | \mathbf{k}, u \rangle|^2 - |\langle \mathbf{k}, o | l_x | \mathbf{k}, u \rangle|^2}{\varepsilon_{\mathbf{k},u} - \varepsilon_{\mathbf{k},o}}, \tag{1}$$

where $|\mathbf{k}, o\rangle$ and $|\mathbf{k}, u\rangle$ represent occupied and unoccupied states with the wave vector $\mathbf{k}$ and $\varepsilon_{\mathbf{k},o(u)}$ the respective eigenvalue. The l_z and l_x are the angular momentum operators of z- and x-components, respectively. The formula involves vertical (same $\mathbf{k}$) coupling between occupied and unoccupied states and their eigenvalue difference. As such difference becomes smaller, the contribution becomes more important in MAE. At the numerator in equation (1), coupling between the same magnetic angular momentum (d_{xz}–d_{yz}, d_{xy}–$\mathrm{d}_{x^2-y^2}$) contributes to the element by l_z, while those between neighboring magnetic angular momentum ($\mathrm{d}_{3z^2-r^2}$–d_{yz}, d_{xy}–d_{xz}, d_{yz}–$\mathrm{d}_{x^2-y^2}$) to the element by l_x. Consequently, the former and latter will contribute to a positive and negative MAE, respectively.

In order to investigate the possibility of MAE, we draw band dispersions with angular orbital component marking, as shown in Figs. 6 and 7. The angular orbital component in the band structure implies the possibility of contribution to positive MAE due to $3\mathrm{d}_{xy}$ and $3\mathrm{d}_{x^2-y^2}$ orbital coupling below and above the Fermi level, for example, at the $\frac{1}{3}$ of $\bar{\mathrm{M}}$ and $\bar{\mathrm{X}}$ in Fig. 6 and coupling between $3\mathrm{d}_{xy}$ and $3\mathrm{d}_{x^2-y^2}$ near $\bar{\mathrm{M}}$ in Fig. 7. These couplings are very near in energy scale, therefore we can predict that the couplings have significant effect in MAE. This property could be a candidate of the reason why the magnetization is perpendicular to the interface plane [3], in addition to the discussion that the hybridization of $3\mathrm{d}_{3z^2-r^2}$ with oxygen 2p orbital can enhance

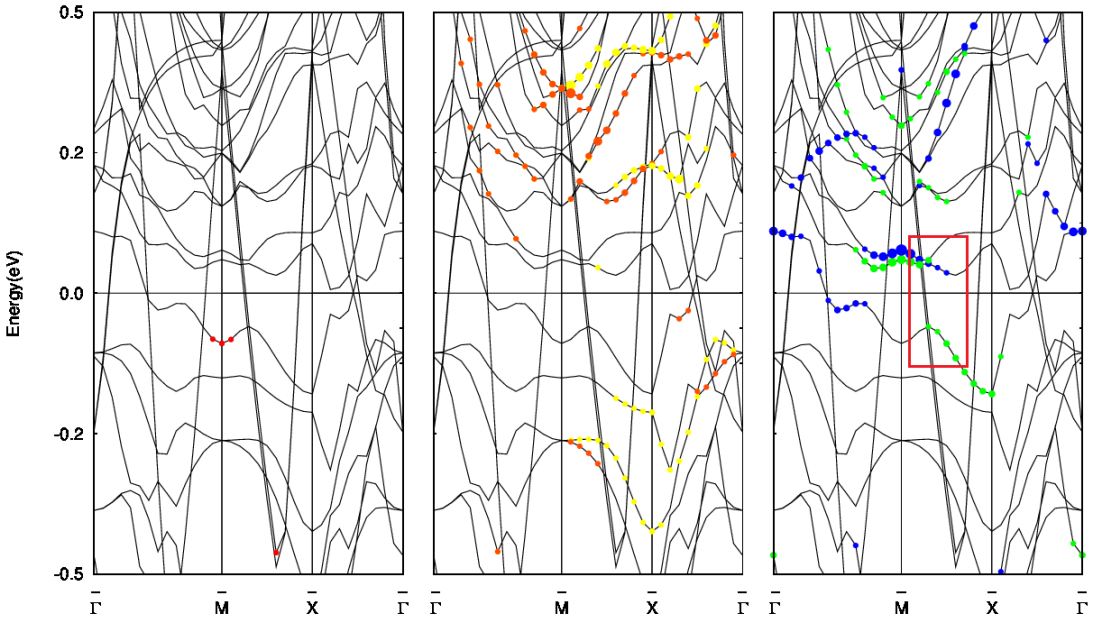

Figure 6: Band dispersion in model A with a_{Fe}. The colored symbol indicates the component of angular orbitals on Fe1; red symbol represents $3d_{3z^2-r^2}$ in the left panel, orange $3d_{xz}$, yellow $3d_{yz}$ in the middle panel, blue $3d_{xy}$, green $3d_{x^2z^2}$ in the right panel.

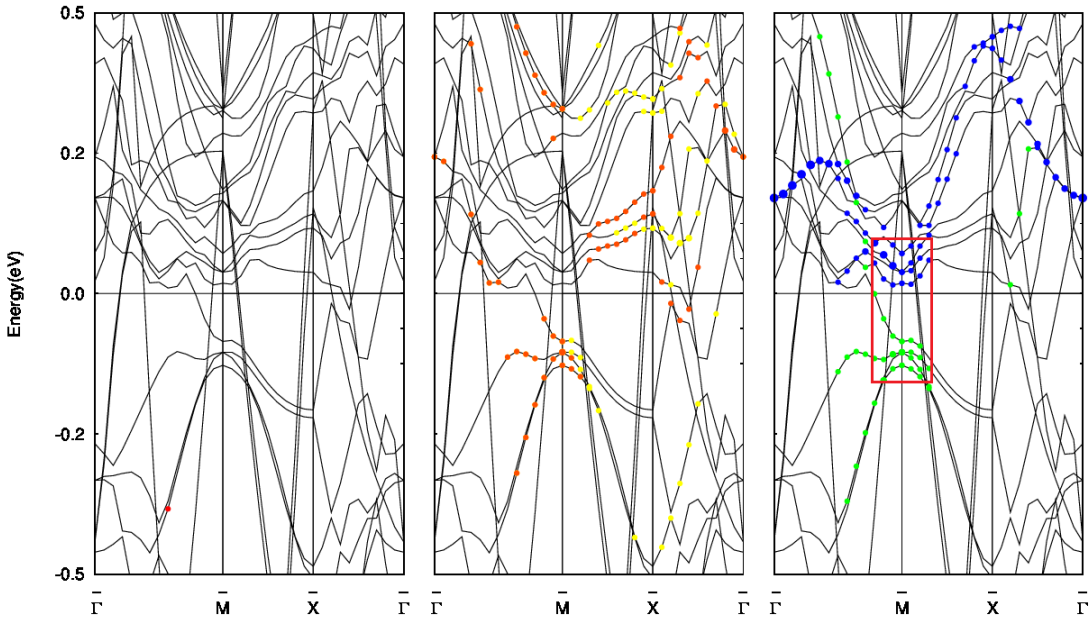

Figure 7: Band dispersion in model B with a_{Fe}. The colored symbols indicate the component of angular orbitals on Fe1; red represents $3d_{3z^2-r2}$, orange $3d_{xz}$, yellow $3d_{yz}$, blue $3d_{xy}$, green $3d_{x^2z^2}$.

the favor of perpendicular magnetic anisotropy [17].

4 Summary

We have investigated FeCo/MgO interface properties by using the first-principles electronic structure calculation. The optimized structure has been obtained, showing the contracting movement of Co to the Fe substrate. Our result indicates that the Co impurity prefers the situation surrounded by Fe rather than bonded with O at the interface. We discussed the possible origin of perpendicular magnetic anisotropy by analyzing the angular component in vicinity of the Fermi level. However, estimation of the practical MAE value at FeCo/MgO interface is left in a future study in which the spin-orbit interaction is taken in electronic structure calculation. Although we obtained the preferable movement of Co at the interface, effect of the impurity has been unclear in the relation with Fe electronic structure. The detail investigation is needed.

References

[1] T. Maruyama et al. (2009). Large voltage-induced magnetic anisotropy change in a few atomic layers of iron. *Nature Nanotech.*, **4**, 158.

[2] Y. Shiota et al. (2009). Voltage-Assisted Magnetization Switching in Ultrathin Fe_80Co_20 Alloy Layers. *Appl. Phys. Exp.*, **2**, 063001.

[3] S. Ikeda et al. (2008). Tunnel magnetoresistance of 604% at 300 K by suppression of Ta diffusion in CoFeB/MgO/CoFeB pseudo-spin-valves annealed at high temperature. *Appl. Phys. Lett.* , **93**, 082508.

[4] M. Tsujikawa, S. Haraguchi, T. Oda, Y. Miura, and M. Shirai (2011). A comparative ab initio study on electric-field dependence of magnetic anisotropy in MgO/Fe/Pt and MgO/Fe/Au films. *J. Appl. Phys.*, **109**, 07C107.

[5] K. Nakamura et al. (2010). Electric field-induced change in magnetocrystalline anisotropy in ferromagnetic transition-metal thin films. *J. Phys.; Conf. Ser.*, **200**, 302051.

[6] W. Kohn and L. J. Sham (1965). Self-Consistent Equations Including Exchange and Correlation Effects. *Phys. Rev.* , **140**, A1133.

[7] D. Vanderbilt (1990). Soft self-consistent pseudopotentials in a generalized eigenvalue formalism. *Phys. Rev. B*, **41**, 7892.

[8] K. Lasasonen, A. Pasquarello, R. Car, C. Lee, D. Vanderbilt (1993). Car-Parinello molecular dynamics with Vanderbilt ultrasoft pseudopotentials *Physical Review B*, **47**, 16

[9] J. P. Perdew et al. (1992). Atoms, molecules, solids, and surfaces: Applications of the generalized gradient approximation for exchange and correlation. *Phys. Rev. B*, **46**, 6671.

[10] M. Otani and O. Sugino (2006). First-principles calculations of charged surfaces and interfaces: A plane-wave nonrepeated slab approach. *Phys. Rev. B*, **73**, 115407.

[11] K. Nakamura, T. Akiyama, T. Ito, M. Weinert, A. J. Freeman (2010). Role of an interfacial FeO layer in the electric-field-driven switching of magnetocrystalline anisotropy at the Fe/MgO interface. *Phys. Rev. B*, **81**, 220409(R).

[12] T. Li and A. J. Freeman (1991). Giant monolayer magnetization of Fe and MgO:A nearly ideal two-dementional magnetic system. *Phys. Rev. B*, **43**, 780.

[13] E. G. Moroni, G. Kresse, and J. Hafner (1997). Ultrasoft pseudopotentials applied to magnetic Fe, Co, and Ni: From atoms to solids. *Phys. Rev. B*, **56**, 15629.

[14] I. M. L. Billas, J. A. Becker, A. Chatelain, and Walt A. de Heer (1993). Magnetic Moments of Iron Clusters with 25 to 700 Atoms and Their Dependence on Temperature. *Phys. Rev. Lett.*, **71**, 4067.

[15] R. Wu and A. J. Freeman (1999). Spin-orbit induced magnetic phenomena in bulk metals and their surfaces and interfaces. *J. Mag. Mag. Mat.*, **200**, 498.

[16] D. S. Wang, R. Wu, and A. J. Freeman (1993). First-principles theory of surface magnetocrystalline anisotropy and the diatomic-pair model. *Phys. Rev. B*, **47**, 14932.

[17] R. Shimabukuro, K. Nakamura, T. Akiyama, T. Ito (2010). Electric field effects on magnetocrystalline anisotropy in ferromagnetic Fe monolayers. *Physica E*, **42**, 1014.